JOURNAL OF ENVIRONMENTAL SCIENCES 93 (2020) 48–56

Available online at www.sciencedirect.com

ScienceDirect

www.elsevier.com/locate/jes

JES JOURNAL OF ENVIRONMENTAL SCIENCES

www.jesc.ac.cn

Environmental factors affecting degradation of perfluorooctanoic acid (PFOA) by In_2O_3 nanoparticles

Weilan Zhang[1], *Harry Efstathiadis*[2], *Lingyun Li*[3], *Yanna Liang*[1,*]

[1] *Department of Environmental and Sustainable Engineering, University at Albany, SUNY, Albany, NY 12222, USA*
[2] *Department of Nanoengineering, SUNY Polytechnic Institute, Albany, NY 12203, USA*
[3] *New York State Department of Health, Division of Environmental Health Sciences, Wadsworth Center, Albany, NY 12237, USA*

ARTICLE INFO

Article history:
Received 22 January 2020
Revised 21 February 2020
Accepted 28 February 2020
Available online 4 April 2020

Keywords:
Perfluorooctanoic acid (PFOA)
Nanophotocatalyst
Degradation
Defluorination
Optimization

ABSTRACT

Nanophotocatalysts have shown great potential for degrading poly- and perfluorinated substances (PFAS). In light of the fact that most of these catalysts were studied in pure water, this study was designed to elucidate effects from common environmental factors on decomposing and defluorinating perfluorooctanoic acid (PFOA) by In_2O_3 nanoparticles. Results from this work demonstrated that among the seven parameters, pH, sulfate, chloride, H_2O_2, In_2O_3 dose, NOM and O_2, the first four had statistically significant negative effects on PFOA degradation. Since PFOA is a strong acid, the best condition leading to the highest PFOA removal was identified for two pH ranges. When pH was between 4 and 8, the optimal condition was: pH = 4.2; sulfate = 5.00 mg/L; chloride = 20.43 mg/L; H_2O_2 = 0 mmol/L. Under this condition, PFOA decomposition and defluorination were 55.22 and 23.56%, respectively. When pH was between 2 and 6, the optimal condition was: pH = 2; sulfate = 5.00 mg/L; chloride = 27.31 mg/L; H_2O_2 = 0 mmol/L. With this condition, the modeled PFOA decomposition was 97.59% with a defluorination of approximately 100%. These predicted results were all confirmed by experimental data. Thus, In_2O_3 nanoparticles can be used for degrading PFOA in aqueous solutions. This approach works best when the target contaminated water contains low concentrations of NOM, sulfate and chloride and at a low pH.

Introduction

Perfluorooctanoic acid (PFOA) has unique physicochemical properties including oil and water repellency, temperature resistance, friction reduction, and is hence used globally in a wide variety of industrial applications and consumer products (Hekster et al., 2003; Herzke et al., 2012; Seow, 2013). The main source of PFOA in the environment is the manufacturing of ammonium perfluorooctanoate (APFO) and its subsequent use in fluoropolymer production (Pistocchi and Loos, 2009). The persistent nature of PFOA, however, has a "double-edged sword" effect, which makes this compound difficult to be degraded in the natural environment. The median half-life for PFOA was determined to be 2.7 years (Li et al., 2018). When this chemical was exposed to strong sunlight at the top of Mt. Mauna Kea (4200 m) in Hawaii, USA, its concentration decreased 5% after 106 days (Taniyasu et al., 2013). Thus, due to its persistence and resistance to degradation, release of PFOA to the environment can result in its occurrence in natural water bodies (Fujii et al., 2007; Benford et al., 2008; Ahrens and Bundschuh, 2014), and posing risks to human health (Kannan et al., 2004; DeWitt et al., 2012; Grandjean and Clapp, 2015). Several reports have already shown that PFOA was detected at high frequency in many river basins that are important sources of drinking water in the USA (Post et al., 2012). Although there is currently no maximum contaminant level established for PFOA, EPA has issued a

* Corresponding author.
E-mail address: yliang3@albany.edu (Y. Liang).

https://doi.org/10.1016/j.jes.2020.02.028
1001-0742/

health advisory level of 70 parts per trillion for this compound (https://www.epa.gov/ground-water-and-drinking-water/drinking-water-health-advisories-pfoa-and-pfos).

Currently, sorption is the only approach used commercially to remove PFOA from contaminated water (Ross et al., 2018). During the process of sorbent regeneration, more than 90% of PFOA sorbed on the sorbents (e.g., hydrogel-based sorbents, permanently confined micelle arrays) can be concentrated in the regenerant or still bottom (Wang et al., 2014; Huang et al., 2018). PFOA concentration in the regenerant can reach 96 mg/L (Lin et al., 2018). Thus, besides the need to dispose the exhausted sorbents, the concentrated waste streams derived from sorbent regeneration need to be handled properly to avoid secondary contamination. In addition, sorption may be challenged by shorter breakthrough time and increased cost for heavily contaminated water, such as wastewater generated from the photolithographic process in the semiconductor industry. The concentration of PFOA in such wastewater was estimated to be about 1000 mg/L (Lampert et al., 2007; Rattanaoudom et al., 2012). Therefore, approaches rather than sorption need to be evaluated.

Photocatalysis is an advanced technology for the removal of organic pollutants from aqueous systems (Nakata and Fujishima, 2012). Decomposition of aqueous PFOA under UV irradiation has been demonstrated to be effective by using TiO_2, Ga_2O_3, and In_2O_3 based photocatalysts (da Silva et al., 2017; Wang et al., 2017). Among them, In_2O_3 based nanophotocatalysts showed the best performance on PFOA decomposition (Li et al., 2012a, 2012b, 2013a; Li et al., 2013b, 2014; da Silva et al., 2017). PFOA was reported to be decomposed by nanosized In_2O_3 under UV light through a step-by-step approach (Li et al., 2012a, 2012b; Jiang et al., 2016). Firstly, photogenerated holes (h_{vb}^+) on the In_2O_3 surface can take electrons from the absorbed PFO^- ($C_7F_{15}COO^-$) and produce $C_7F_{15}COO\cdot$ radicals. The $C_7F_{15}COO\cdot$ radicals are then transformed to $C_7F_{15}\cdot$ radicals after Kolbe decarboxylation reaction. The $C_7F_{15}\cdot$ radicals can quickly react with ·OH or HOO· radicals and form thermodynamically unstable $C_7F_{15}OH$. Afterwards, the $C_7F_{15}OH$ undergoes hydrolysis and HF elimination, forming $C_6F_{13}COO^-$. Similarly, $C_6F_{13}COO^-$ can be decomposed into $C_5F_{11}COO^-$ by repeating the same process, and finally mineralizes to CO_2 and fluoride ions. The intermediates during the decomposition process are perfluoroheptanoic acid (PFHpA), perfluorohexanoic acid (PFHxA), perfluoropentanoic acid (PFPeA), perfluorobutanoic acid (PFBA), and trifluoroacetic acid (TFA) (Li et al., 2012b). Since the photocatalytic reaction takes place on the surface of In_2O_3, efforts have been devoted to increasing the specific surface area of the nanosized In_2O_3 particles. Li et al. (2012b) synthesized the In_2O_3 nanoporous nanosphere with a uniform size of around 100 nm and an average specific surface area of 39.0 m^2/g. The decomposition half-life of PFOA by using the In_2O_3 nanoporous nanosphere was 7.1 min under a low-pressure mercury lamp (23 W). Later on, Li et al. (2013b) shortened the decomposition half-life of PFOA to 5.4 min by modifying the structure of In_2O_3 to porous microsphere. The advantages of In_2O_3 nanostructures, such as shorter reaction time, lower energy consumption, and higher surface reactivity and PFOA removal efficiency make the photocatalysis a promising technology for removing PFOA from aqueous solutions.

At the time of writing, most of the studies using photocatalysts have focused on degrading target compounds in pure water. In the real world, PFOA usually coexists with other ions and/or compounds, such as chloride, sulfate, and natural organic matter (NOM) in the concentrated waste streams derived from sorbent regeneration or industry wastewater. NOM and pH have been reported to affect the photocatalytic activities of In_2O_3 nanostructures by influencing the adsorption process and consuming radicals in aqueous systems (Li et al., 2012a). The inorganic anions, such as chloride and sulfate are also known to inhibit the surface activity of the photocatalyst by diminishing the colloidal stability of photocatalysts, reducing the surface contact between the target chemical and the photocatalyst, and scavenging the radicals and photogenerated holes that can decompose pollutants (Fujishima et al., 2000; Kumar and Pandey, 2017). Dissolved O_2 in water is usually considered as an electron acceptor in photocatalysis reaction and can reduce the recombination of excited electron and holes on photocatalyst surface (Kumar and Pandey, 2017). H_2O_2 is reported to significantly increase the production of $O_2\bullet^-$ and OH• radicals during photocatalysis process (Hirakawa and Nosaka, 2002). Thus, O_2 and H_2O_2 are often employed to improve the performance of selected photocatalysts. Although the effect of individual factor (i.e. photocatalyst dose, pH, chloride, sulfate, NOM, H_2O_2, O_2) on the decomposition of organic pollutions has been investigated previously, information on the interactive and collective effects of these factors on PFOA removal from heavily contaminated water using In_2O_3 nanostructures under UV irradiation is scarce. Thus, the objectives of this study are to: (1) understand the effect of different parameters on PFOA degradation by In_2O_3 nanoparticles; (2) identify the optimal conditions leading to maximal PFOA degradation and defluorination; and (3) arrive mathematical equations for predicting PFOA removal within the studied boundary.

1. Materials and methods

1.1. Chemical reagents and laboratory materials

The abbreviations, suppliers, and purities of the chemicals used in this study can be found in Appendix A Table S1. The low-pressure mercury UV lamp (15 W, 4400 μW/cm^2) was purchased from Analytik Jena (Jena, Germany). Materials used for cleanup and quantification of the samples included 15-mL polypropylene (PP) tubes (Corning, Tewksbury, MA, USA), 2.0-mL PP vials and caps (Thermo Scientific, Waltham, MA, US) for samples ready to be analyzed by LC/MS/MS, and 0.2 μm nylon membrane filter (Thermo Scientific, Waltham, MA, USA). The 250-mL PP bottles for photocatalytic reactions were purchased from Nalgene (Rochester, NY, USA).

1.2. In_2O_3 nanoparticle synthesis and characterization

The In_2O_3 nanoparticles were prepared through a solvothermal method reported by Li et al. (2012b). Briefly, seven hundred mg of $In(NO_3)_3\cdot H_2O$ was first dissolved in 34 mL of ethanol. Subsequently, 34 mL of 1,2-propanediamine was dropped into the solution with continuous stirring. The mixture was then transferred into a 100-mL Teflon-lined stainless-steel autoclave (Boshi Electronic Instrument, China). The autoclave was sealed and heated at 180 °C for 16 hr. The white precipitate (i.e., $In(OH)_3$) were collected and washed with ethanol twice followed by deionized water for another two times. After washing, the white precipitate was calcinated at 500 °C for 2 hr in air. The light-yellow products (In_2O_3 nanoparticles) were then collected for later use.

The morphology of the samples was observed using a LEO 1550 Scanning Electron Microscope (SEM) (Zeiss, Thornwood, NY) equipped with a Bruker XFlash 6061 EDS (Bruker, Billerica, MA, USA). The X-ray powder diffraction (XRD) patterns of the synthesized In_2O_3 nanoparticles were taken in a Bruker D8 Advance X-ray powder diffractometer (Bruker, Billerica, MA, USA).

1.3. Reaction procedure

The photocatalytic decomposition of PFOA was conducted in a tubular PP bottle reactor under UV irradiation. A low-pressure

Table 1 – Two-Level factorial design with results.

No.	In_2O_3 dose (mg/L)	pH	Sulfate (mg/L)	Chloride (mg/L)	NOM (mg/L)	H_2O_2 (mM)	O_2	Decomposition (%)
1	H	L	L	L	L	0	No O_2	52.77
2	H	L	H	H	L	0	O_2	8.37
3	L	L	H	H	L	H	No O_2	8.99
4	H	H	L	H	L	0	O_2	2.54
5	L	L	L	H	H	0	No O_2	0.77
6	L	L	L	L	L	H	O_2	39.93
7	H	L	L	H	L	H	No O_2	34.32
8	L	H	L	L	L	0	No O_2	33.46
9	H	L	H	L	L	H	O_2	11.H
H	L	L	H	H	H	H	O_2	3.45
11	L	H	H	H	L	0	O_2	18.11
12	L	H	H	L	H	H	No O_2	9.05
13	H	L	H	H	H	0	No O_2	0.72
14	H	H	H	H	L	H	No O_2	13.04
15	H	H	H	H	H	H	O_2	1.47
16	H	L	H	L	H	H	No O_2	19.67
17	L	H	L	H	H	H	O_2	14.11
18	H	H	H	L	L	0	No O_2	30.65
19	L	L	L	L	H	H	No O_2	26.09
H	H	L	L	H	H	H	O_2	13.69
21	L	L	L	H	L	0	O_2	26.57
22	H	H	L	L	H	H	No O_2	25.11
23	H	H	L	H	H	0	No O_2	2.12
24	H	L	L	L	H	0	O_2	31.91
25	H	H	H	L	H	0	O_2	3.14
26	H	H	L	L	L	H	O_2	15.08
27	L	H	L	H	L	H	No O_2	9.46
28	L	H	H	H	H	0	No O_2	4.42
29	L	H	H	L	L	H	O_2	H.22
30	L	H	L	L	H	0	O_2	19.84
31	L	L	H	L	H	0	O_2	35.15
32	L	L	H	L	L	0	No O_2	23.49

Note: L stands for the low level value, H stands for the high level value.

mercury lamp (15 W) emitting 254 nm UV light was placed in the center of the reactor with quartz tube protection (Appendix A Fig. S1). PFOA solution at 30 mg/L was used in this work to simulate PFOA in concentrated wastewater derived from other PFAS removal processes, such as sorption. Effect of UV degradation of PFOA was tested first without the addition of any In_2O_3. For those with the photocatalyst, 0.05 g of In_2O_3 nanoparticles were suspended in 100 mL of PFOA solution in a sonicator for 15 min. The pH of the solution was then adjusted by using HCl or NaOH. Chloride, sulfate, and NOM were introduced by adding NaCl, K_2SO4, and Suwannee River NOM (RO isolation) (International Humic Substances Society, Denver, CO, USA) to the solution. Before irradiation, the suspensions were stirred in the dark for 30 min to ensure the establishment of adsorption–desorption equilibrium. On an average, the concentration of PFOA after this 30-min equilibrium was 93.2% of what was added initially. After turning on the UV lamp, oxygen gas was continuously bubbled into the reactor at a flow rate of 60 mL/min during the reaction according to the experimental design. After 90 min, the UV light was turned off. Withdrawn subsamples of 10 mL were passed through 0.2-μm filters to remove the photocatalyst for subsequent analysis. To avoid potential PFOA sorption to the filters, the first 5 mL filtrate were discarded.

1.4. *Experiment design*

To screen the critical factors that affect PFOA decomposition, a two-level factorial design through using Design of Expert (DOE, Stat-Ease, Inc. Minneapolis, MN) was adopted. A total of 7 parameters were evaluated (Table 1): In_2O_3 dose, 100 or 1000 mg/L; (2) solution pH, 4 or 9; (3) sulfate, 0 or 250 mg/L; (4) chloride, 0 or 250 mg/L; (5) NOM, 0 or 10 mg/L; (6) H_2O_2, 0 or 20 mmol/L; and (7) O_2, with or without O_2 bubbling. The upper limit for sulfate and chloride was set at 250 mg/L since this is the secondary maximum contaminant level set by US EPA for drinking water. The rationale behind this selection was that the developed technology, if successful, could be used for degrading PFOA from contaminated drinking water. We do realize though, concentration of PFOA in drinking water may seldom reach the level targeted in this study. The addition of H_2O_2 in photocatalytic reactions for improving organic pollutant removal was reported to be up to 10 mmol/L (Elmolla and Chaudhuri, 2010). In order to see its effect on PFOA removal, we intended to use it at 20 mmol/L as the highest concentration. The response was PFOA decomposition. According to this design, a total of 32 runs (Table 1) was set up and conducted following the above reaction procedure. Percentages of PFOA degradation from all runs were subject to statistical analyses through use of the DOE software.

Results from the screening test indicated that among the 7 parameters tested, four had statistically significant effect on PFOA decomposition. To identify the optimal value for each of the four: solution pH, concentration of sulfate, chloride, and H_2O_2, Response Surface Methodology (RSM) through use of Box–Behnken design was adopted (Table 2 and 3). The primary response was percentage of PFOA disappearance with percentage of PFOA defluorination as the secondary response.

Table 2 – Box–Behnken design with results (pH = 4–8).

Run	pH	Sulfate (mg/L)	Chloride (mg/L)	H_2O_2 (mmol/L)	Decomposition (%)	Defluorination (%)
1	L	M	M	M	11.64	3.30
2	M	M	M	L	13.33	2.26
3	L	L	M	H	46.28	23.93
4	M	M	H	M	5.09	2.59
5	H	M	H	M	3.00	1.34
6	L	M	H	L	10.38	2.65
7	L	H	L	M	19.68	5.16
8	L	H	M	L	13.87	2.74
9	L	H	H	M	13.22	2.01
10	M	M	M	H	6.32	2.04
11	L	M	H	H	1.68	2.02
12	H	M	M	L	6.41	1.66
13	M	L	M	M	11.24	2.33
14	H	L	M	M	1.41	1.79
15	L	L	L	M	59.72	17.41
16	L	H	M	H	9.46	2.44
17	H	M	M	H	7.04	1.98
18	L	M	L	H	12.13	3.55
19	L	M	M	M	6.20	2.37
20	M	M	L	M	16.89	5.95
21	L	L	M	L	50.02	18.69
22	L	M	L	L	29.81	7.02
23	H	H	M	M	7.61	1.47
24	M	H	M	M	12.45	2.05
25	L	M	M	M	2.86	1.77
26	L	L	H	M	26.76	11.34
27	H	M	L	M	11.54	3.52
28	L	M	M	M	12.97	2.82
29	L	M	M	M	12.04	1.95

Note: L stands for the low level value, M stands for the medium level value, H stands for the high level value.

For solution pH, the lower and upper limit was 4 and 8 or 2 and 6. Regarding sulfate and chloride, 0 and 250 mg/L served as the low and upper concentrations. H_2O_2 was tested at 0 or 20 mmol/L. Once the lower and upper values were set, the DOE software automatically generated a middle value for each factor. Thus, in Table 2 and 3, each factor was studied at three levels.

After all the runs were finished and results analyzed, the DOE software was used to find models that fit the experimental data. All models went through a series of analysis of variance (ANOVA), lack of fit, precision and diagnostics. Statistically significant models were then used for optimization analysis, through which the DOE software gave optimal value for each target parameter.

To verify the mathematical models, experiments were performed adopting the values predicted by the DOE software. Results of PFOA degradation and defluorination were compared with those given by the software. Confirmation tests were terminated until the experimental results matched those predicted values.

1.5. *Sample analysis*

Quantification of PFOA was performed using a 1290 Infinity II LC system coupled with a 6470 Triple Quad Mass Spectrometer (Agilent Technologies, Santa Clara, CA, USA). Before analysis, internal standard, ^{13}C-PFOA was added to all standards and samples to yield a concentration of 10 pg/μL. An Agilent ZORBAX Eclipse Plus C18 (3.0 × 50 mm, 1.8 μm) analytical column and an Agilent Eclipse Plus C18 (4.6 × 50 mm, 3.5 μm) delay column were used at 50 °C. The injection volume of samples was 5 μL. Solvent A was 5 mmol/L ammonium acetate in water and solvent B was 5 mmol/L ammonium acetate in 95% methanol. The flow rate of the mobile phase was 0.4 mL/min. The LC gradient elution started at 90% A, decreased to 70% A at 2 min, then decreased to 5% at 14 min, followed by another decrease to 0% A at 14.5 min and held for 2 min before reverting to original conditions. The MS instrument was operated in Agilent Jet Stream electrospray negative ionization mode and dynamic multiple reaction monitoring (dMRM) mode. The retention time, fragmentor voltage, and collision energy were 11.85 min, 60 eV, and 4 eV, respectively.

The fluoride ion concentration in the samples were determined using an Orion ionplus Sure-Flow fluoride Electrode (Thermo Scientific, Waltham, MA, USA).

The per- and polyfluoroalkyl substance (PFAS) non-targeted analysis was performed using a HPLC system (Shimadzu, model LC-20ADXR) coupled to a high-resolution MS (SCIEX TripleTOF MS 6600 system with DuoSpray™ source) in negative mode. Before analysis, the HPLC MS system was calibrated using the external standard calibrant delivery system (CDS). Poroshell EC–C18 HPLC column was used for separation of analytes (Agilent, 2.7 μm particle size, 2.1 × 100 mm). The injection volume of samples was 5 μL. Solvent A was 2 mmol/L ammonium acetate in water/methanol mixture (ratio is 90/10) and solvent B was 2 mmol/L ammonium acetate in 100% methanol. The mobile phase flow rate was 0.35 mL/min and column temperature was at 35 °C. The LC gradient elution was started at 10% B, increased to 100% B in 6 min, kept to 100% B for 2 min, then back to 10% B at 8 min and held for 2 min for resetting the column. The MS instrument was operated in electrospray negative ionization mode for high resolution MS and MS/MS acquisition. Information dependent acquisition (IDA) was used for a TOF-MS survey scan from 100 to 2000 Da (250 mS) and 5 dependent MS/MS scans were applied using standard collision energy (CE) = 35 V with collision

Table 3 – Box–Behnken design with results (pH = 2–6).

Run	pH	Sulfate (mg/L)	Chloride (mg/L)	H_2O_2 (mmol/L)	Decomposition (%)	Defluorination (%)
1	M	M	M	M	11.64	3.30
2	H	M	M	L	13.33	2.26
3	M	L	M	H	46.28	23.93
4	H	M	H	M	5.09	2.59
5	L	M	H	M	2.19	2.78
6	M	M	H	L	10.38	2.65
7	M	H	L	M	19.68	5.16
8	M	H	M	L	13.87	2.74
9	M	H	H	M	13.22	2.01
10	H	M	M	H	6.32	2.04
11	M	M	H	H	1.68	2.02
12	L	M	M	L	18.51	2.83
13	H	L	M	M	11.24	2.33
14	L	L	M	M	89.47	97.91
15	M	L	L	M	59.72	17.41
16	M	H	M	H	9.46	2.44
17	L	M	M	H	0.76	2.97
18	M	M	L	H	12.13	3.55
19	M	M	M	M	6.20	2.37
20	H	M	L	M	16.89	5.95
21	M	L	M	L	50.02	18.69
22	M	M	L	L	29.81	7.02
23	L	H	M	M	13.02	2.26
24	H	H	M	M	12.45	2.05
25	M	M	M	M	2.86	1.77
26	M	L	H	M	26.76	11.34
27	L	M	L	M	12.55	2.73
28	M	M	M	M	12.97	2.82
29	M	M	M	M	12.04	1.95

Note: L stands for the low level value, M stands for the medium level value, H stands for the high level value.

energy spread (CES) ± 15 V. Data was acquired using Analyst Software (version 1.6.1). Data processing used PeakView software and MultiQuant software (version 2.1). Customized PFAS compound library was established using PFAS standards purchased from Wellington Laboratories (Guelph, Ontario).

1.6. *Statistical and graphical analysis*

Design-Expert version 10.0.7.0. (Stat-Ease Inc., Minneapolis, USA) software was used for statistical analysis and graphical presentation of the experimental data. ANOVA was performed with respect to a 95% confidence level. The quality of the models was evaluated by coefficient of determination (R^2), adjusted R^2 (R^2_{adj}), and predicted R^2 (R^2_{pred}).

2. Results

2.1. *Characterization of In_2O_3 nanoparticles*

The SEM image and EDS elemental spectrum (Fig. 1a and b) showed that the In_2O_3 particles were at nano-scale and formed the porous structure as indicated in the previous report (Li et al., 2013b). The negligible difference between the experimental and simulated patterns of In_2O_3 (Fig. 1c) demonstrated the high purity of the synthesized In_2O_3 nanoparticles.

2.2. *Two-level factorial design*

Based on the half-normal probability plot (Fig. 2), all seven parameters had negative effect on PFOA decomposition (%).The

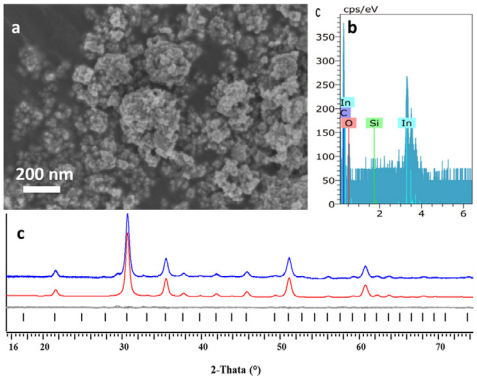

Fig. 1 – (a) SEM image of In_2O_3 nanoparticles, (b) the corresponding EDS elemental spectrum, and (c) X-ray powder diffraction pattern and Le Bail fit for In_2O_3. Blue and red lines in (c) are the experimental and simulated patterns of In_2O_3, respectively. Gray line shows the difference between the experimental and simulated patterns.

largest negative effect came from chloride with a relative contribution of 31.37% (Appendix A Table S2). The largest positive effect was from the interaction between chloride and H_2O_2 with a relative contribution of 5.59%. ANOVA (Appendix A Table S3) indicated that pH, sulfate, chloride, NOM, and interactions between In_2O_3 and O_2, pH and sulfate, chloride and H_2O_2 had statistically significant effects with $p < 0.05$. Con-

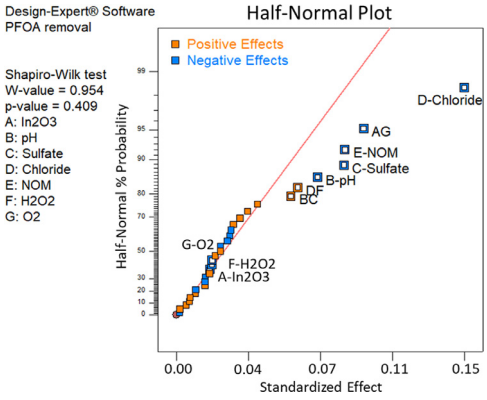

Fig. 2 – Half normal probability plot for perfluorooctanoic acid decomposition in screening test. The hollow squares represent the selected factors. BC stands for the interaction between pH (B) and Sulfate (C). DF stands for the interaction between Chloride (D) and H_2O_2 (F).

sidering these results, four out of the seven parameters were selected as the most important factors for PFOA decomposition: pH and concentration of sulfate, chloride, and H_2O_2. Non-significant factors including dose of In_2O_3 and O_2 were eliminated from further investigations. Since NOM had a negative effect with high relative contribution, lower concentration of NOM should always be beneficial for PFOA degradation. Thus, NOM was eliminated from further experiments as well. The increase in the photocatalyst dose could result in an increase of reaction sites for PFOA decomposition. However, a further increase in the photocatalyst concentration may lead to lower UV light penetration and thus a decrease of PFOA degradation. Therefore, In_2O_3 at 0.5 g/L, a dosage commonly applied in previous investigations (Li et al., 2012b, 2013b, 2014), was adopted in the following experiments.

2.3. *Box–Behnken design*

Since PFOA is a strong acid with a pKa of −0.21 (Steinle-Darling and Reinhard, 2008) or 0–4 (Goss and Arp, 2009), we chose two pH ranges for optimization: 2–6 and 4–8. When the pH was between 4 and 8 (Appendix A Table S4), a reduced cubic model was found to fit the results of PFOA degradation well with a p value < 0.0001. All factors except pH were statistically significant with p values less than 0.05. Regarding PFOA defluorination at the same pH range (Appendix A Table S5), pH was also a statistically significant factor. These analyses led to Eqs. (1) and (2) that can be used to calculate percentage of PFOA degradation and defluorination, respectively. It needs to be noted that the percentage of PFOA degradation only considered those degraded after the UV light was turned on. Thus, PFOA sorbed to In_2O_3 nanoparticles before the catalytic reaction started was not counted in the calculation.

$$\begin{aligned}&\text{PFOA decomposition}(\%)\\&= 109.8285 - 11.9506 \times \text{pH} - 1 \times \text{Sulfate} - 0.1128\\&\times \text{Chloride} - 0.3409\times H_2O_2 + 0.1342 \times \text{pH} \times \text{Sulfate} + 0.0004\\&\times \text{Sulfate}\times\text{Chloride} + 0.0026 \times \text{Sulfate}^2 - 0.0004 \times \text{pH}\\&\times \text{Sulfate}^2 \left(R^2 = 0.9250, R^2_{adj} = 0.8950, R^2_{pred} = 0.7493\right) \quad (1)\end{aligned}$$

$$\begin{aligned}&\text{Ln(PFOA defluorination}(\%))\\&= 5.0224 - 0.3958 \times \text{pH} - 0.0235\times\text{Sulfate} - 0.0098\\&\times \text{Chloride} - 0.0592\times H_2O_2 + 0.0018 \times \text{pH} \times \text{Sulfate}\\&+ 0.0026\times {H_2O_2}^2 \left(R^2 = 0.8419, R^2_{adj} = 0.7787, R^2_{pred} = 0.6071\right)\\&(2)\end{aligned}$$

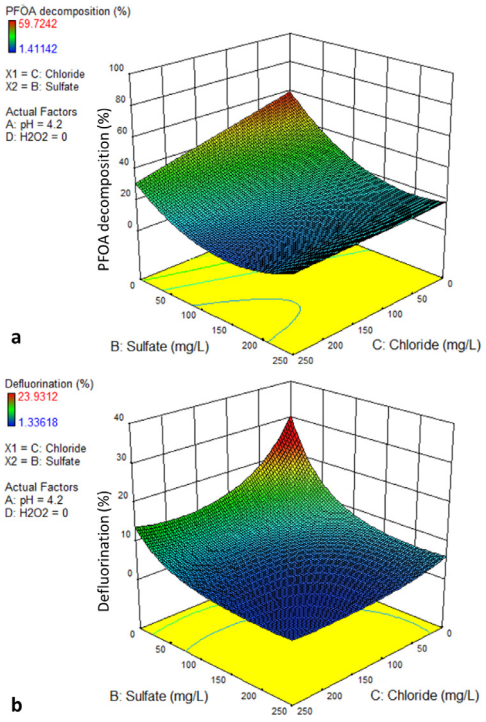

Fig. 3 – 3-D response surface for (a) perfluorooctanoic acid composition and (b) PFOA defluorination at pH = 4–8.

The 3-D response surface (Fig. 3a) showed that PFOA decomposition could reach up to 59% with the decrease of sulfate and chloride concentrations when pH was fixed at 4.2 (the initial pH of PFOA solution at 30 mg/L) and H_2O_2 was set at 0 mmol/L. The 3-D graph on PFOA defluorination demonstrated that the defluorination percentage could be close to 30% under the same conditions (Fig. 3b). In light of the dramatically negative effect of sulfate and chloride on PFOA removal, when conducting the optimization analysis, we considered realistic concentrations of these two anions in environmental matrices. For example, for New York City drinking water, the average detected concentration was 5.1–6.5 mg/L for sulfate and 18–24 mg/L for chloride (Sapienza, 2016, 2017, 2018). For groundwater in Texas, USA, the median concentrations ranged from < 1.5 to 1953 mg/L for sulfate, and from 6 to 1275 mg/L for chloride (Hudak, 2000). Thus, from the list of optimal conditions given by the DOE software, the condition that we selected was: pH = 4.2; sulfate = 5.00 mg/L; chloride = 20.43 mg/L; H_2O_2 = 0 mmol/L. Under this condition, the predicted PFOA decomposition was 55.22% with defluorination of 23.56%. It is noteworthy that without In_2O_3, the same UV light alone decomposed around 3.15% of spiked PFOA at 30 mg/L in 90 min in pure water. These results are in line with what was reported by other researchers, such as Shao et al., 2013) and Li et al. (2012a). Thus, the majority of PFOA degradation we observed in this study was contributed by In_2O_3.

At pH = 2–6, a different set of reduced cubic models was able to fit the measured data regarding PFOA removal and defluorination with p values < 0.0001 (Appendix A Table S6 and S7). The mathematical expressions for PFOA decomposition and defluorination were:

$$\begin{aligned}&\text{PFOA decomposition}(\%)\\&= 144.6651 - 19.5571 \times \text{pH} - 1.4809\\&\times\text{Sulfate} - 0.1140 \times \text{Chloride} - 0.4941\times H_2O_2 + 0.2429 \times \text{pH}\end{aligned}$$

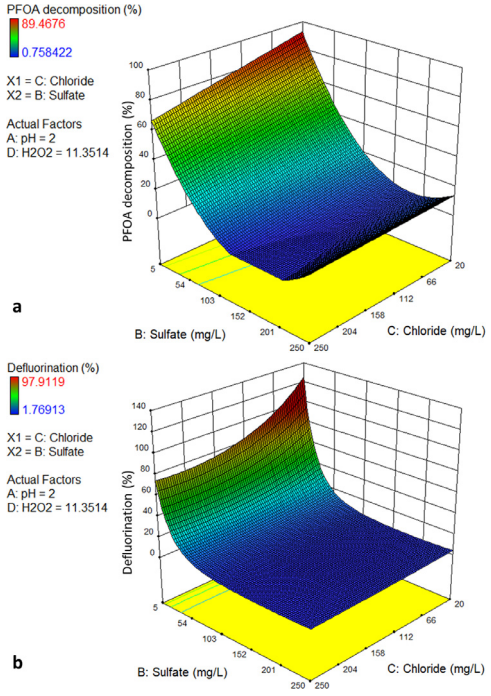

Fig. 4 – 3-D response surface for (a) perfluorooctanoic acid decomposition and (b) PFOA defluorination at pH = 2–6.

$$\times \text{Sulfate} + 0.0004 \times \text{Sulfate} \times \text{Chloride} + 0.0039 \times \text{Sulfate}^2 - 0.0007 \times \text{pH} \times \text{Sulfate}^2$$
$$\left(R^2 = 0.9673, R^2_{adj} = 0.9543, R^2_{pred} = 0.9194\right) \quad (3)$$

$$\text{Ln(PFOAdefluorination(\%))} = 6.9902 - 0.9343 \times \text{pH} - 0.0670 \times \text{Sulfate} - 0.0058 \times \text{Chloride} + 0.0114 \times \text{pH} \times \text{Sulfate} + 0.0002 \times \text{Sulfate}^2 \left(R^2 = 0.9366, R^2_{adj} = 0.9155, R^2_{pred} = 0.8824\right) \quad (4)$$

The 3-D response surface showed that PFOA decomposition and defluorination could both reach 100% with the decrease of sulfate and chloride concentrations when pH was set at 2.0 and H_2O_2 at 0 mmol/L (Fig. 4). Adopting the same rationale we used to arrive optimal condition when pH was between 4 and 8, the optimal condition for the pH range of 2 and 6 was: pH = 2.0; sulfate = 5.00 mg/L; chloride = 27.31 mg/L; H_2O_2 = 0 mmol/L. With these conditions, the predicted PFOA removal was 97.59% with a nearly 100% defluorination.

To verify the modeled results, the optimal conditions were used to perform PFOA degradation. At pH = 4.2, we observed PFOA removal of 53.50% ± 5.01% and defluorination of 21.33% ± 3.71%. When the pH was 2.0, PFOA decomposition and defluorination was 92.20% ± 3.38% and 95.99% ± 5.65%, respectively. Therefore, the models developed from this study could be used to predict PFOA removal and defluorination accurately as long as the conditions were within the ranges detailed above.

2.4. *PFAS non-target analysis*

The non-target analysis was used to detect PFOA degradation products. As shown in Fig. 5, under the optimal condition with pH = 4.2, the detected intermediates were perfluoroheptanoic acid (PFHpA), perfluorohexanoic acid (PFHxA), and perfluoropentanoic acid (PFPeA). When the pH was 2, only PFHpA

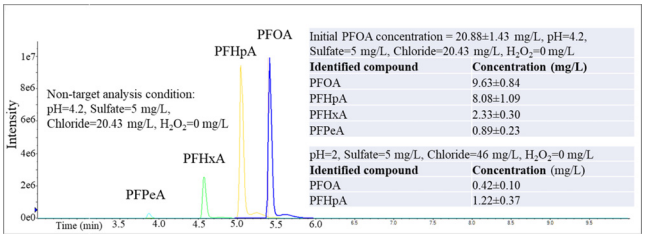

Fig. 5 – Perfluorinated substances non-target analysis of the photocatalytic reaction products.

was detected, indicating that most of PFOA was decomposed to F^- and CO_2. This is consistent with the high defluorination (95.99% ± 5.65%) achieved at this pH.

3. Discussion

As mentioned above, sorption between PFOA and In_2O_3 nanoparticles is the prerequisite for the photocatalytic reactions to initiate and the electrostatic interaction between PFOA and the nano-photocatalyst plays an important role in the adsorption process. The point of zero charge of In_2O_3 nanostructures was reported to be around 7 or 8.7 (Kosmulski, 2001). The lower the pH value is, the more positive the In_2O_3 surface could be. On the other hand, as described above, PFOA, as a strong acid, has a pK_a reported to be between −0.21 and 4 (Steinle-Darling and Reinhard, 2008) (Goss and Arp, 2009). When the solution pH is higher than the pK_a, the majority of PFOA should be in the dissociated form, the anions and with the increase of pH, the concentration of PFO^- should be increased. Thus, considering the electrostatic interactions, low pH is beneficial for PFOA sorption.

In this study, the highest PFOA degradation and defluorination took place when the pH was 2.0, the lowest pH studied in the experiment designs. At pH=8.0, the PFOA removal and defluorination were lower than 10% in all tests, indicating the negative effect of alkaline pH. It needs to be noted that at 30 mg/L in pure water, the PFOA solution has a pH around 4.2. For lowering the pH to 4.0, the addition of Cl^- from HCl was negligible. To lower the pH to 2.0, 364.63 mg/L of Cl^- needs to be supplemented. Thus, for all the pHs we studied, only pH at 2.0 was affected by pH adjustment.

Keeping this in mind, we still proceeded with data analysis based on the initial design table (Table 3). Once statistically significant models are identified, we conducted experiments to validate the predicted results. It turned out that the model for the pH 2–6 range could be confirmed even though some actual Cl^- concentrations in the reactor were much higher than what we considered. Therefore, even though Cl^- had a negative effect on PFOA degradation, the pH effect was much more significant. At pH 2.0, the positive effect from this low pH on PFOA degradation masked the negative effect from Cl^-. Freshwater in the natural environment typically has a pH between 6.5 and 9 as stipulated by US EPA (https://www.epa.gov/caddis-vol2/caddis-volume-2-sources-stressors-responses-ph). Thus, whether to lower pH and to what extent will be case by case.

Besides pH, other factors, such as NOM, sulfate, chloride and H_2O_2 can affect the efficiency of photocatalytic reactions. NOM can greatly inhibit the photocatalytic activities of In_2O_3 nanostructures (Li et al., 2012a; Ross et al., 2018). The inhibition of PFOA decomposition could be attributed to two aspects: competitive adsorption of PFOA on In_2O_3 surface and radical consumption. The significantly negative effect of NOM

on PFOA degradation observed in this study correlated well with reported inhibition, implying the importance of NOM reduction to facilitate better PFOA degradation. Typical NOM removal techniques, including coagulation with subsequent floc separation, oxidation followed by biofiltration, and sorption processes such as chemisorption (ion exchange) and physical adsorption (activated carbon) (Ødegaard et al., 2010), may need to be used before PFOA treatment.

The inorganic anions, such as sulfate and chloride are known to inhibit the surface activity of photocatalyst. The presence of these anions increases the ionic strength of the solution and can cause aggregation of the nano-photocatalysts (French et al., 2009). The formation of photocatalyst aggregates can significantly decrease the specific surface area of the nanoparticles, hence reducing the surface contact between the target chemical and the photocatalysts and decreasing PFOA decomposition efficiency as observed in this study.

A few studies have shown that sulfate can improve the photocatalytic activities of TiO_2-based photocatalysts (Wiszniowski et al., 2003; Zhang et al., 2016), which is contradictory to what we saw in this investigation. Zhang et al. (2016) proposed that the sulfate anions on the TiO_2 surface could capture the photon-generated electrons and increase the formation of oxygen ions ($\bullet O_2^-$) and hydroxyl radicals (•OH), resulting in the improvement of TiO_2 photocatalytic activity. However, it has been proved that direct hole oxidation has significantly higher PFOA decomposition efficiency than $\bullet O_2^-$ and •OH oxidation (Kutsuna et al., 2006; Vecitis et al., 2009). Thus, the negative effect of sulfate on PFOA degradation is in line with most of the published literature. But further mechanistic investigation is needed to explain the discrepancies reported by different studies.

As shown in this study, chloride had similar effect on PFOA degradation as sulfate. Matthews and McEvoy (1992) proposed that chloride can scavenge radicals and photogenerated holes (h^+) by the following reactions:

$$Cl^- + \bullet OH \rightarrow Cl\bullet + OH^- \quad (5)$$

$$Cl^- + h^+ \rightarrow Cl\bullet \quad (6)$$

h^+ is the major species that is responsible for PFOA decomposition. The chlorine radical (Cl•), although is capable of oxidizing organic pollutants, it would selectively react more with electron-rich compounds and may negatively affect the decomposition rates and pathways of organic contaminants by h^+, such as PFOA.(Kumar and Pandey, 2017).

H_2O_2 can be employed to improve the performance of selected photocatalysts (Hirakawa and Nosaka, 2002). Previous research showed that H_2O_2 can accept the conduction band electrons (photogenerated electrons) and yield hydroxyl radicals and hydroxyl ions (Elmolla and Chaudhuri, 2010):

$$H_2O_2 + e^- \rightarrow \bullet OH + OH^- \quad (7)$$

The hydroxyl ions can then react with the photogenerated holes (h^+) to form additional •OH, which have the ability to degrade organic compounds. H_2O_2 can also effectively degrade NOM in water under UV irradiation (Wang et al., 2006; Vilhunen et al., 2010), and further improve the performance of photocatalysis. Moreover, Varanasi et al. (2018) reported that chlorine radicals (Cl•) can effectively degrade dissolved NOM. In this study, the interactions between H_2O_2 and chloride had positive effect on PFOA decomposition in the screening test (Fig. 2). The degradation of NOM by generated Cl• and hydroxyl •OH in the solution might contribute to the positive effect. When NOM was eliminated from the solution as indicated in the Box-Behnken design, H_2O_2 had negative effect on PFOA decomposition, possibly due to consumption of h^+ by H_2O_2 and the low decomposition efficiency of •OH for PFOA.

It is noteworthy that the highest PFOA decomposition efficiency of 53.50% ± 5.01% at pH = 4.2 was lower than what was reported before. Li et al. (2013b) demonstrated complete degradation of PFOA at 30 mg/L using the same In_2O_3 nanostructures under UV irradiation (15 W, 254 nm) within 20 min. In that study, the solution pH was not adjusted and it should be around 4.2. Wang and Zhang (2011) reported that the system with TiO_2 nanoparticles and oxalic acid could efficiently decompose 86.7% of PFOA (10 mg/L, no pH adjustment) within 180 min. Li et al. (2016) modified TiO_2 with Pt and Pd nanoparticles and decomposed 94.2% and 100% of PFOA (60 mg/L at pH=3), respectively, after 7 hr of UV irradiation. Panchangam et al. (2018) found that TiO_2-graphene nanocomposites (200 mg/L) could photocatalytically decompose more than 90% of aqueous PFOA (5 mg/L, no pH adjustment) after 8 hr of UV irradiation. Shao et al. (2013) synthesized β-Ga_2O_3 with a sheaf-like nanostructure, which can completely decompose PFOA (500 μg/L, no pH adjustment) within 45 min. Zhao et al. (2015) synthesized β-Ga_2O_3 nanorod by a one-step microwave hydrothermal method without any subsequent heat treatments. The decomposition and defluorination of PFOA (100 mg/L, no pH adjustment) within 90 min were 98.8% and 56.2%, respectively. In our case, such high degradation was only achieved at pH=2 within 90 min. In addition, at pH of 4.2, degradation of PFOA was incomplete. The identification of the degradation intermediates: PFHpA, PFHxA, and PFPeA, points to a need for further investigation in terms of their environmental risks.

4. Conclusions

A response surface methodology coupled with a two-level factorial design was applied to establish predictive models in order to evaluate PFOA decomposition and defluorination upon exposure to In_2O_3 nanoparticles and UV. The present study showed that both PFOA degradation and defluorination can be satisfactorily computed using reduced cubic models. Results from this study demonstrated that In_2O_3 nanoparticles can be used for degrading PFOA in aqueous solution. This approach works best for waste streams containing high concentration of PFOA and low concentrations of NOM, sulfate and chloride at low pH. The significance of this study lies in the facts: (1) that the boundary of this treatment system is defined; (2) the optimal treatment conditions are identified and (3) models predicting PFOA degradation and defluorination are available as long as the relevant parameters are within the ranges reported here.

Whether the use of nano-photocatalyst for PFOA degradation can be applied to surface water and drinking water depends strongly on PFOA removal efficiency at low concentration and the water chemistry. In addition, the use of In_2O_3 nanoparticles in suspension could cause problems for downstream processes. All of these deserve to be investigated extensively before this removal approach can be used in the field.

Acknowledgment

The authors wish to thank Dr. Haixiang Han at the Chemistry Department at University at Albany, SUNY for assisting the XRD analysis of the synthesized nanoparticles. The authors are also grateful for the funding provided by University at Albany, State University of New York.

Appendix A. Supplementary data

Supplementary material associated with this article can be found, in the online version, at doi:10.1016/j.jes.2020.02.028.

REFERENCES

Ahrens, L., Bundschuh, M., 2014. Fate and effects of poly-and perfluoroalkyl substances in the aquatic environment: a review. Environ. Toxicol. Chem. 33, 1921–1929.

Benford, D., De Boer, J., Carere, A., Di Domenico, A., Johansson, N., Schrenk, D., et al., 2008. Opinion of the scientific panel on contaminants in the food chain on perfluorooctane sulfonate (PFOS), perfluorooctanoic acid (PFOA) and their salts. EFSA J. 653, 1–131.

da Silva, F.L., Laitinen, T., Pirilä, M., Keiski, R.L., Ojala, S., 2017. Photocatalytic degradation of perfluorooctanoic acid (PFOA) from wastewaters by TiO2, In_2O_3 and Ga_2O_3 catalysts. Top. Catal. 60, 1345–1358.

DeWitt, J.C., Peden-Adams, M.M., Keller, J.M., Germolec, D.R., 2012. Immunotoxicity of perfluorinated compounds: recent developments. Toxicol. Pathol. 40, 300–311.

Elmolla, E.S., Chaudhuri, M., 2010. Photocatalytic degradation of amoxicillin, ampicillin and cloxacillin antibiotics in aqueous solution using UV/TiO_2 and UV/H_2O_2/TiO_2 photocatalysis. Desalination 252, 46–52.

French, R.A., Jacobson, A.R., Kim, B., Isley, S.L., Penn, R.L., Baveye, P.C., 2009. Influence of ionic strength, pH, and cation valence on aggregation kinetics of titanium dioxide nanoparticles. Environ. Sci. Technol. 43, 1354–1359.

Fujii, S., Polprasert, C., Tanaka, S., Lien, H., Pham, N., Qiu, Y., 2007. New POPs in the water environment: distribution, bioaccumulation and treatment of perfluorinated compounds – a review paper. J. Water Supp.: Res. Technol. – AQUA 56, 313–326.

Fujishima, A., Rao, T.N., Tryk, D.A., 2000. Titanium dioxide photocatalysis. J. Photochem. Photobiol. C 1, 1–21.

Goss, K.-U., Arp, H.P.H., 2009. Comment on "Experimental pKa determination for perfluorooctanoic acid (PFOA) and the potential impact of pKa concentration dependence on laboratory-measured partitioning phenomena and envrionmental modeling". Environ. Sci. Technol. 43, 5150–5151.

Grandjean, P., Clapp, R., 2015. Perfluorinated alkyl substances: emerging insights into health risks. New Sol. 25, 147–163.

Hekster, F.M., Laane, R.W., de Voogt, P., 2003. Environmental and toxicity effects of perfluoroalkylated substances. Reviews of Environmental Contamination and Toxicology. Springer, pp. 99–121.

Herzke, D., Olsson, E., Posner, S., 2012. Perfluoroalkyl and polyfluoroalkyl substances (PFASs) in consumer products in Norway – a pilot study. Chemosphere 88, 980–987.

Hirakawa, T., Nosaka, Y., 2002. Properties of O2•-and OH• formed in TiO_2 aqueous suspensions by photocatalytic reaction and the influence of H_2O_2 and some ions. Langmuir 18, 3247–3254.

Huang, P.-J., Hwangbo, M., Chen, Z., Liu, Y., Kameoka, J., Chu, K.-H., 2018. Reusable functionalized hydrogel sorbents for removing long-and short-chain perfluoroalkyl acids (PFAAs) and Genx from aqueous solution. ACS Omega 3, 17447–17455.

Hudak, P.F., 2000. Sulfate and chloride concentrations in Texas aquifers. Environ. Int. 26, 55–61.

Jiang, F., Zhao, H., Chen, H., Xu, C., Chen, J., 2016. Enhancement of photocatalytic decomposition of perfluorooctanoic acid on CeO_2/In_2O_3. RSC Adv. 6, 72015–72021.

Kannan, K., Corsolini, S., Falandysz, J., Fillmann, G., Kumar, K.S., Loganathan, B.G., et al., 2004. Perfluorooctanesulfonate and related fluorochemicals in human blood from several countries. Environ. Sci. Technol. 38, 4489–4495.

Kosmulski, M., 2001. Pristine points of zero charge of gallium and indium oxides. J. Colloid Interface Sci. 238, 225–227.

Kumar, A., Pandey, G., 2017. A review on the factors affecting the photocatalytic degradation of hazardous materials. Mater. Sci. Eng. Int. J. 1, 106–114.

Kutsuna, S., Nagaoka, Y., Takeuchi, K., Hori, H., 2006. TiO_2-induced heterogeneous photodegradation of a fluorotelomer alcohol in air. Environ. Sci. Technol. 40, 6824–6829.

Lampert, D.J., Frisch, M.A., Speitel Jr, G.E., 2007. Removal of perfluorooctanoic acid and perfluorooctane sulfonate from wastewater by ion exchange. Pract. Period. Hazard. Toxic, Radioact. Waste Manag. 11, 60–68.

Li, M., Yu, Z., Liu, Q., Sun, L., Huang, W., 2016. Photocatalytic decomposition of perfluorooctanoic acid by noble metallic nanoparticles modified TiO_2. Chem. Eng. J. 286, 232–238.

Li, X., Zhang, P., Jin, L., Shao, T., Li, Z., Cao, J., 2012a. Efficient photocatalytic decomposition of perfluorooctanoic acid by indium oxide and its mechanism. Environ. Sci. Technol. 46, 5528–5534.

Li, Y., Fletcher, T., Mucs, D., Scott, K., Lindh, C.H., Tallving, P., et al., 2018. Half-lives of PFOS, PFHXS and PFOA after end of exposure to contaminated drinking water. Occup. Environ. Med. 75, 46–51.

Li, Z., Zhang, P., Li, J., Shao, T., Jin, L., 2013a. Synthesis of In_2O_3-graphene composites and their photocatalytic performance towards perfluorooctanoic acid decomposition. J. Photochem. Photobiol. A: Chem. 271, 111–116.

Li, Z., Zhang, P., Li, J., Shao, T., Wang, J., Jin, L., 2014. Synthesis of In_2O_3 porous nanoplates for photocatalytic decomposition of perfluorooctanoic acid (PFOA). Catal. Commun. 43, 42–46.

Li, Z., Zhang, P., Shao, T., Li, X., 2012b. In_2O_3 nanoporous nanosphere: a highly efficient photocatalyst for decomposition of perfluorooctanoic acid. Appl. Catal. B 125, 350–357.

Li, Z., Zhang, P., Shao, T., Wang, J., Jin, L., Li, X., 2013b. Different nanostructured In_2O_3 for photocatalytic decomposition of perfluorooctanoic acid (PFOA). J. Hazard. Mater. 260, 40–46.

Lin, H., Niu, J., Liang, S., Wang, C., Wang, Y., Jin, F., et al., 2018. Development of macroporous Magnéli phase Ti_4O_7 ceramic materials: as an efficient anode for mineralization of poly- and perfluoroalkyl substances. Chem. Eng. J. 354, 1058–1067.

Matthews, R.W., McEvoy, S.R., 1992. A comparison of 254nm and 350nm excitation of TiO_2 in simple photocatalytic reactors. J. Photochem. Photobiol. A: Chem. 66, 355–366.

Nakata, K., Fujishima, A., 2012. TiO_2 photocatalysis: design and applications. J. Photochem. Photobiol. C 13, 169–189.

Ødegaard, H., Østerhus, S., Melin, E., Eikebrokk, B., 2010. NOM removal technologies – Norwegian experiences. Drink. Water Eng. Sci. 3, 1–9.

Panchangam, S.C., Yellatur, C.S., Yang, J.-S., Loka, S.S., Lin, A.Y.C., Vemula, V., 2018. Facile fabrication of TiO_2-graphene nanocomposites (TGNCs) for the efficient photocatalytic oxidation of perfluorooctanoic acid (PFOA). J. Environ. Chem. Eng. 6, 6359–6369.

Pistocchi, A., Loos, R., 2009. A map of European emissions and concentrations of PFOS and PFOA. Environ. Sci. Technol. 43, 9237–9244.

Post, G.B., Cohn, P.D., Cooper, K.R., 2012. Perfluorooctanoic acid (PFOA), an emerging drinking water contaminant: a critical review of recent literature. Environ. Res. 116, 93–117.

Rattanaoudom, R., Visvanathan, C., Boontanon, S.K., 2012. Removal of concentrated PFOS and PFOA in synthetic industrial wastewater by powder activated carbon and hydrotalcite. J. Water Sustain. 2, 245–258.

Ross, I., McDonough, J., Miles, J., Storch, P., Thelakkat Kochunarayanan, P., Kalve, E., et al., 2018. A review of emerging technologies for remediation of PFASs. Remed. J. 28, 101–126.

Sapienza, V., 2016. New York City 2016 drinking water supply and quality report. NYC Environmental Protection, New York.

Sapienza, V., 2017. New York City 2017 drinking water supply and quality report. NYC Environmental Protection, New York.

Sapienza, V., 2018. New York City 2018 drinking water supply and quality report. NYC Environmental Protection, New York.

Seow, J., 2013. Fire Fighting Foams with Perfluorochemicals-Environmental Review. Hemming Information Services.

Shao, T., Zhang, P., Jin, L., Li, Z., 2013. Photocatalytic decomposition of perfluorooctanoic acid in pure water and sewage water by nanostructured gallium oxide. Appl. Catal. B: Environ. 142, 654–661.

Steinle-Darling, E., Reinhard, M., 2008. Nanofiltration for trace organic contaminant removal: structure, solution, and membrane fouling effects on the rejection of perfluorochemicals. Environ. Sci. Technol. 42, 5292–5297.

Taniyasu, S., Yamashita, N., Yamazaki, E., Petrick, G., Kannan, K., 2013. The environmental photolysis of perfluorooctanesulfonate, perfluorooctanoate, and related fluorochemicals. Chemosphere 90, 1686–1692.

Varanasi, L., Coscarelli, E., Khaksari, M., Mazzoleni, L.R., Minakata, D., 2018. Transformations of dissolved organic matter induced by UV photolysis, hydroxyl radicals, chlorine radicals, and sulfate radicals in aqueous-phase UV-Based advanced oxidation processes. Water Res. 135, 22–30.

Vecitis, C.D., Park, H., Cheng, J., Mader, B.T., Hoffmann, M.R., 2009. Treatment technologies for aqueous perfluorooctanesulfonate (PFOS) and perfluorooctanoate (PFOA). Front. Environ. Sci. Eng. China 3, 129–151.

Vilhunen, S., Vilve, M., Vepsäläinen, M., Sillanpää, M., 2010. Removal of organic matter from a variety of water matrices by UV photolysis and UV/H2O2 method. J. Hazard. Mater. 179, 776–782.

Wang, F., Lu, X., Shih, K.M., Wang, P., Li, X., 2014. Removal of perfluoroalkyl sulfonates (PFAS) from aqueous solution using permanently confined micelle arrays (PCMAs). Sep. Purif. Technol. 138, 7–12.

Wang, G., Liao, C.-H., Chen, H.-W., Yang, H., 2006. Characteristics of natural organic matter degradation in water by UV/H2O2 treatment. Environ. Technol. 27, 277–287.

Wang, S., Yang, Q., Chen, F., Sun, J., Luo, K., Yao, F., et al., 2017. Photocatalytic degradation of perfluorooctanoic acid and perfluorooctane sulfonate in water: a critical review. Chem. Eng. J. 328, 927–942.

Wang, Y., Zhang, P., 2011. Photocatalytic decomposition of perfluorooctanoic acid (PFOA) by TiO_2 in the presence of oxalic acid. J. Hazard. Mater. 192, 1869–1875.

Wiszniowski, J., Robert, D., Surmacz-Gorska, J., Miksch, K., Weber, J.-V., 2003. Photocatalytic mineralization of humic acids with TiO_2: effect of pH, sulfate and chloride anions. Int. J. Photoenergy 5, 69–74.

Zhang, J., Wang, X., Wang, J., Wang, J., Ji, Z., 2016. Effect of sulfate ions on the crystallization and photocatalytic activity of TiO_2/diatomite composite photocatalyst. Chem. Phys. Lett. 643, 53–60.

Zhao, B., Li, X., Yang, L., Wang, F., Li, J., Xia, W., et al., 2015. ß-Ga_2O_3 nanorod synthesis with a one-step microwave irradiation hydrothermal method and its efficient photocatalytic degradation for perfluorooctanoic acid. Photochem. Photobiol. 91, 42–47.